doi.org/10.1002/cbdv.202100785

FULL PAPER

CHEMISTRY & BIODIVERSITY

Biochemical Characterization and Antimicrobial Activity against Some Human or Phyto-Pathogens of New Diazonium Heterocyclic Metal Complexes

Mohamed S. El-Attar,[a] Hazem S. Elshafie,*[b] Sadeek A. Sadeek,[a] Ahmed F. El-Farargy,[a] Sameh I. El-Desoky,[c] Walaa H. El-Shwiniy,[d] and Ippolito Camele*[b]

[a] Department of Chemistry, Faculty of Science, Zagazig University, Zagazig, 44519, Egypt
[b] School of Agricultural, Forestry, Food and Environmental Sciences, University of Basilicata, Viale dell'Ateneo Lucano 10, Potenza, 85100, Italy, e-mail: ippolito.camele@unibas.it; hs.elshafie@gmail.com
[c] Regional Joint Laboratory, Directorate of Health Affairs, Zagazig, 44515, Egypt
[d] Department of Chemistry, College of Science, University of Bisha, Bisha, 61922, Saudi Arabia

String of vanadium (IV), zirconium (IV), palladium (II), platinum (IV) and uranium (VI) chelates of 2-cyano-2-[(2-nitrophenyl)hydrazono]thioacetamide (Cnphta) were prepared and characterized by physicochemical, spectroscopic and thermal analyses. The formulae of the isolated solid complexes were assigned as $[VO(Cnphta)_2(H_2O)]SO_4\cdot 5H_2O$ (**1**), $[ZrO(Cnphta)_2(H_2O)]Cl_2\cdot 4H_2O$ (**2**), $[Pd(Cnphta)_2]Cl_2$ (**3**), $[Pt(Cnphta)_2Cl_2]Cl_2$ (**4**) and $[UO_2(Cnphta)_2](NO_3)_2\cdot 5H_2O$ (**5**). The infrared assignments clearly showed that Cnphta ligand coordinated as a bidentate feature through the hydrazono nitrogen and the thioacetamide nitrogen for V(IV), Zr(IV) and U(VI) but displayed different behavior for Pd(II) and Pt(IV). Results of the molar conductivities measurements showed that the metal complexes were electrolytes in contrast with Cnphta ligand. The interpretation, mathematical analysis and evaluation of kinetic parameters were also carried out. In addition, the studied ligand and its new chelates were tested for their antimicrobial activity against some human or phytopathogenic microorganisms. The new metal complexes explicated promising antibacterial activity against all tested bacteria especially *Staphylococcus aureus* and *Bacillus subtilis*. Regarding the antifungal activity, all metal complexes were able to inhibit the mycelium growth of both tested pathogenic fungi. In particular Zr(IV) and Pt(IV) complexes showed the highest significant fungicidal effect against *A. fumigatus* similar to positive control.

Keywords: Cnphta, metal complexes, spectroscopic, human and phytopathogens, antimicrobial activity.

Introduction

Recently, there is a high interest in a programs targeted at manufacturing of functionally substituted heterocyclic compounds from low-cost raw materials to evaluate them as biodegradable agrochemicals and environmentally friendly and safe pesticides.[1–3] The pharmaceutical importance of organic compounds containing azo group have been found to exhibit a wide range of biological activities like antibacterial, antitumor and as potent local anesthetics.[4,5] Aryl diazonium salts represent a well-known and important group to synthesize heterocyclic compounds that possess many diverse biological activities such as bactericidal, pesticidal, anticonvulsant, anti-inflammatory and antithyroid diseases and tuberculostatic treatment.[6–8] During the last two decades, considerable attention has been paid to the chemistry of the metal complexes of organic heterocyclic compounds containing nitrogen and other donors due to their stability and promising biological activities.[9–15]

The bibliographic research showed that no work has been reported on 2-cyano-2-[(2-

Supporting information for this article is available on the WWW under https://doi.org/10.1002/cbdv.202100785

nitrophenyl)hydrazono]thioacetamide (Cnphta). The objective of this research is to document the synthesis, structural characterization and biological activity of new prepared chalcone metal complexes with V(IV), Zr(IV), Pd(II), Pt(IV) and U(VI) using hetero organic molecule Cnphta. In the present research, Cnphta was prepared via the coupling 2-nitrobenzendiazonium chloride with 2-cyano-ethane-thioamide in presence of sodium acetate in ethanol.[4] The chemical formulas and structures of Cnphta (*Figure 1*) and its metal complexes were established via magnetic conductance measurements, elemental analysis, UV/VIS., mass (MS), IR and ^{1}H-NMR spectroscopy as well as thermogravimetric analyses (TG/DTG) and kinetic parameters. The antibacterial activity of the studied Cnphta and the new prepared complexes were evaluated against some human or phyto- pathogenic bacteria *Staphylococcus aureus*, *Bacillus subtilis* (Gram-positive, G+ ve) and *Escherichia coli* and *Pseudomonas aeruginosa* (Gram-negative, G-ve). Whereas the antifungal activity were carried out against *Aspergillus flavus* and *A. fumigatus*.

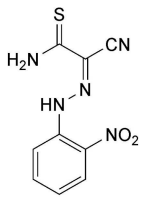

Figure 1. 2-Cyano-2-[(2-nitrophenyl)hydrazono]thioacetamide (Cnphta).

Results and Discussion

The new synthesized chelates of (**1**) V(IV), (**2**) Zr(IV), (**3**) Pd(II), (**4**) Pt(IV) and (**5**) U(VI) with Cnphta are stable in air and insoluble in most of the organic solvents, colored and non-hygroscopic in nature. All the complexes were solvable in dimethyl formamide and dimethyl sulfoxide. The exquisite physical properties and distinctive data of the Cnphta ligand and its chelates were evaluated (*Table 1*). In order to decide whether SO_4^{2-}, Cl^- and NO_3^- anions are coordinated or outside the coordination sphere, the conductance of 1.0×10^{-3} DMSO solutions of the complexes were measured at room temperature (*Table 1*). The observed value for the complex (**1**) is 95.40 $S\,cm^2\,mol^{-1}$ shows 1:1 electrolyte, while (**2**), (**3**), (**4**) and (**5**) complexes with values 150.45, 144.81, 141.17 and 156.36 $S\,cm^2\,mol^{-1}$, respectively, are 1:2 electrolytes.[16] Comparison of the analyses for both the calculated and found data indicates that the compositions of the isolated complexes are coincided with the proposed formulae. The magnetic moment value for the complex (**1**) found at 1.65 B.M reveals the presence of one unpaired electron per V(IV) ion.

IR Absorption Spectra

The IR spectra of Cnphta ligand and its metal complexes are shown in Figure S1 and listed in *Table 2*. The IR spectra of the complexes were used with free ligand for the determination of coordinating sites that may be involved in complexation. All Cnphta complexes showed abroad band in the 3422–3436 cm^{-1} zone, the presence of these bands confirms the presence of water molecules.[17–19]

Table 1. Elemental analysis and physico-analytical data for Cnphta and its metal complexes.

Compounds M.Wt., M.F.	Yield %	M.p./°C	Color	Found (calc.) (%)					Λ ($S\,cm^2\,mol^{-1}$)
				C	H	N	Cl	M	
Cnphta 249.06, $C_9H_7N_5O_2S$	–	228	Yellowish	43.26 (43.36)	2.78 (2.81)	28.01 (28.10)	–	–	–
$[VO(C_9H_7N_5O_2S)_2(H_2O)]SO_4\cdot5H_2O$ 769.13, $VC_{18}H_{26}N_{10}O_{15}S_2$ (**1**)	73	240	Dark -Brown	28.00 (28.08)	3.30 (3.38)	18.08 (18.20)	–	6.52 (6.62)	95.40
$[ZrO(C_9H_7N_5O_2S)_2(H_2O)]Cl_2\cdot4H_2O$ 766.35, $ZrC_{18}H_{24}N_{10}O_{10}S_2Cl_2$ (**2**)	88	247	Yellowish-White	28.10 (28.18)	3.02 (3.13)	18.19 (18.26)	9.21 (9.26)	11.80 (11.90)	150.45
$[Pd(C_9H_7N_5O_2S)_2]Cl_2$ 675.55, $PdC_{18}H_{14}N_{10}O_4S_2Cl_2$ (**3**)	90	210	Black	31.89 (31.97)	2.00 (2.07)	20.57 (20.72)	10.40 (10.50)	15.70 (15.75)	144.81
$[Pt(C_9H_7N_5O_2S)_2Cl_2]Cl_2$ 835.21, $PtC_{18}H_{14}N_{10}O_4S_2Cl_4$ (**4**)	85	180	Orange-Brown	25.76 (25.86)	1.60 (1.67)	16.67 (16.76)	16.90 (17.00)	23.30 (23.35)	141.17
$[UO_2(C_9H_7N_5O_2S)_2](NO_3)_2\cdot5H_2O$ 982.16, $UC_{18}H_{24}N_{12}O_{11}S_2$ (**5**)	80	235	Yellowish-Green	21.88 (21.99)	2.38 (2.44)	17.00 (17.10)	–	24.11 (24.23)	156.36

Table 2. Selected infrared absorption frequencies (cm^{-1}) of Cnphta and its metal complexes.

Compounds	ν(O–H); H_2O	ν(N–H); –NH	ν(N–H); $–NH_2$	ν(C≡N)	ν(C=N)	ν(C=S)	ν(Zr=O)	ν(V=O)	ν_{as}(U=O) and ν_s(U=O)	ν(M–N)
Cnphta	3433s	3322s	3230m	2206m	1604vs	1219vs	–	–	–	–
1	3429s	3310m	3220w	2206m	1604vs	1219vs	–	894vs	–	628s, 574vs
2	3433vs	3311m	3221w	2206m	1604vs	1219vs	811w	–	–	632s, 574s
3	3422m	3321s	3229m	2215w	1611s	1219vs	–	–	–	644ms, 90m
4	3436w	3321s	3229m	2216w	1611s	1219vs	–	–	–	655m, 578vs
5	3433m	3311m	3221w	2206m	1604vs	1219vs	–	–	949vs, 864ms	655vw, 628s

s = strong, w = weak, v = very, m = medium, ν = stretching.

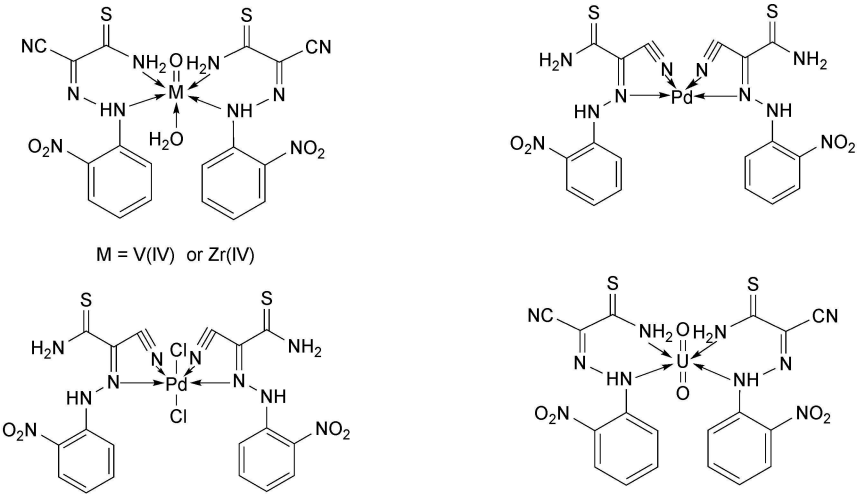

Figure 2. The coordination mode of V(IV), Zr(IV), Pd(II), Pt(IV) and U(VI) with Cnphta.

The Cnphta ligand showed stretching vibration bands attributed to NH, NH_2, CN, C=N and C=S at 3322, 3230, 2206, 1604 and 1219 cm^{-1}, respectively.[19] The shift of –NH (~3311 cm^{-1}) and $–NH_2$ (~3221 cm^{-1}) to lower frequency values with different intensities for the complexes spectra of (**1**), (**2**) and (**5**) proved that Cnphta chelated through the $N_{hydrazono}$ and $N_{thioacetamide}$ entities with V(IV), Zr(IV) and U-(VI).[18,19] The spectra of (**3**) and (**4**) chelates signaling the change of ν(C≡N) (~2215 cm^{-1}) and ν(C=N) (1611 cm^{-1}) to higher frequency specified the participation of the C=N and C≡N units in interaction with metal ions. New bands matched to ν(M–N) vibration supporting the pointed out the mode of coordination (*Figure 2*) at 628 and 574 cm^{-1} for (**1**), at 632 and 574 cm^{-1} for (**2**), at 644 and 590 cm^{-1} for (**3**), at 655 and 578 cm^{-1} for (**4**) and at 655 and 628 cm^{-1} for (**5**) (*Table 2*) which are absent in the spectrum of Cnphta. The infrared spectra of the synthesized complexes display changes in the aromatic ring vibrations in comparison to the corresponding absorption bands for free ligand. According to the proposed structure for the complexes under investigation (*Figure 2*), the four nitrogen atoms of Cnphta ligand positioned in the equatorial regions around the metal ions generate a plane of six membered rings with C_{2v} symmetry. The C_{2v} complex, $[UO_2(Cnphta)_2]^{2+}$ was suggested to demonstrate 147 vibrational fundamentals, which all are monodegenerate.[19–22] These are distributed between A_1, A_2, B_1 and B_2 motions; all are IR and Raman active, except for the A_2 modes which are only Raman active. The uranyl moiety has two stretching vibration peaks (asymmetric and symmetrical) at 949 and 864 cm^{-1}.[20–23] The calculated bond length and force constant values are 1.71 Å and 281.96 Nm^{-1} according to the known method.[24,25] The results are very consistent with the data found for other di-oxo-uranium(VI) chelates.

Electronic Spectroscopy of the Complexes

Figure S2 depicts the electronic solid reflection spectra of Cnphta and its chelates in the wavelength scale from 200 to 800 nm. It can be seen that free Cnphta

ligand reflected at 231 and 249 nm may be attributed to π-π* transition and the second band observed at 380 nm is assigned to n-π* transitions (*Table 3*).[26] The complexes reflection bands were shifted to higher (bathochromic shift) and lower (hypsochromic shift) positions, as well as the absence of the band at 231 nm and the inclusion of new bands from 400 nm to 517 nm that can be allocated to the ligand to metal charge-transfer suggested the creation of their chelates.[27,28] Furthermore, the chelates (**1**), (**3**) and (**4**) provided new bands corresponding to the d-d transitions which showed from 524 to 578 nm.[29]

^{1}H-NMR Spectra

^{1}H-NMR spectra of Cnphta, (**2**), (**4**) and (**5**) compounds were recorded in (D_6)DMSO (Figure S3 and *Table 4*). The protons of –NH and $–NH_2$ signals of (**2**), (**4**) and (**5**) chelates were marginally differentiated in the Cnphta spectrum, and it was observed at: 11.55–11.12 ppm (s, 2H, –NH, D_2O) and at: 9.77–10.08 ppm (s, 4H, $–NH_2$, D_2O), implying that the Cnphta ligand was chelated in (**2**) and (**5**) complexes through the two nitrogen atoms of –NH and $–NH_2$. These protons peaks in the (**4**) complex, which were found at 11.12 and 10.04 ppm, showed no measurable difference with Cnphta, indicating that the two groups are not coordinated. Furthermore, owing to the existence of water molecules in the complexes, the ^{1}H-NMR spectra for (**2**), (**4**) and (**5**) chelates indicate a novel peak in the range 3.00–4.15 ppm. Matching the Cnphta's key peaks to their complexes, the intensity of –CH aromatic protons signals was increased and reported in the range δ: 6.89–8.40 ppm (m, 8H, Ar–H).[30]

Mass Spectra

Mass spectral analyses of representative chelates were performed to validate the formula weights suggested on the basis of elemental analysis. The mass spectra of Cnphta, (**1**), (**2**), (**3**), (**4**) and (**5**) compounds depicted in (Figure S4), showed the parent peaks at *m/z* (%) 249 (57.93%), 769 (30.47%), 765 (35.50%), 674 (70.63%), 833 (44.80%) and 982 (66.66%), respectively. *Scheme 1* demonstrates Cnphta's fragmentation mode. Where, at *m/z* = 249 (57.93%) allocated to the molecular ion

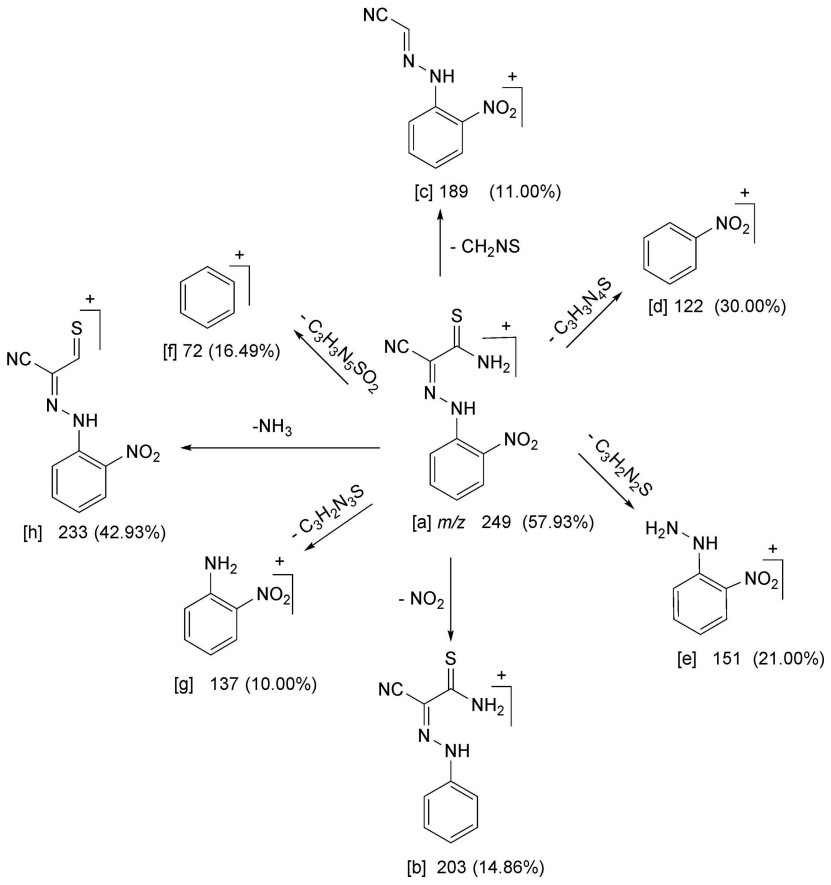

Scheme 1. Fragmentation pattern of Cnphta.

Table 3. UV/VIS spectral data of Cnphta and its metal complexes.

Assignments (nm)	Cnphta	Cnphta complexes with				
		V(IV)	Zr(IV)	Pd(II)	Pt(IV)	U(VI)
π-π* transitions	231, 249	240	244	251	262	227
n-π* transitions	380	379, 391	281, 370	374, 392	281, 374	272
Ligand-metal charge transfer	–	400, 517	426	429, 469, 487	449, 494	419
d-d transitions	–	530, 549, 578	–	543, 572, 577	524, 543, 577	–

Table 4. Selected ^{1}H-NMR data of Cnphta and its metal complexes **2**, **4** and **5**.

Compounds	δH; H_2O	δH; –CH aromatic	δH; –NH amine	δH; –NH hydrazid
Cnphta	–	6.89–8.01	10.04	11.12
2	3.00, 3.33	7.29–8.42	9.78, 10.08	11.56
4	3.14, 4.15	6.92–8.35	10.04	11.12
5	3.01, 3.42	7.28–8.40	9.77, 10.07	11.55
2 in D_2O	3.01, 3.42	7.28–8.40	–	–

peak [a] losses NO_2 to produce [b] at $m/z=203$ (14.86%), also it losses CH_2NS to give fragment [c] at $m/z=189$ (11.00%). The molecular ion peak [a] losses $C_3H_3N_4S$ to produce [d] at $m/z=122$ (30.00%) and it also losses $C_3H_2N_2S$ to produce fragment [e] at $m/z=151$ (21.00%). It losses $C_3H_3N_5SO_2$ to produce [f] at $m/z=72$ (16.49%) and losses $C_3H_2N_3S$ to produce fragment [g] at $m/z=137$ (10.00%). The molecular ion peak [a] losses NH_2 to produce fragment [h] at $m/z=233$ (42.93%). *Scheme 2* manifest the fragmentation manner of (**5**) complex as representative case. Where at $m/z=982$ (66.66%) allocated to the molecular ion peak [a] losses N_2O_4 to produce [b] at $m/z=890$ (50.00%) and it losses $C_{12}H_8N_2O_4$ to produce [c] at $m/z=738$ (23.55%). The molecular ion peak [a] losses $C_6H_4NO_2$ to produce [d] at $m/z=860$ (28.77%) and it losses C_2N_2 to produce [e] at $m/z=930$ (19.00%). The molecular ion peak [a] losses $C_2N_4O_4$ to produce [f] at $m/z=838$ (17.89%) and it losses NO_2 to produce [g] at $m/z=936$ (13.20%).

Thermal Studies

Thermogravimetric analyses for prepared compounds were carried out under N_2 flow to support the proposed formulae and structures (Figure S5). A survey of the literature reveals that the order of decomposition by pyrolysis of the constituents of solid complexes is water, anion, ligand and final residue, corresponding to either metal oxide or free metal. The thermograms of Cnphta showed a thermal stability up to 150 °C then decomposed in one step in the range 150–650 °C with mass loss 99.90% correspond to the loss of $HSCN+3C_2H_2+2CO+2N_2$ (*Table 5*). The data of the thermogram of $[VO(Cnphta)_2(H_2O)]SO_4\cdot 5H_2O$ complex (1) shows that the complex was decomposed with two steps. The first step occurs in the range 50–150 °C with mass loss 11.67% (calc.=11.70%) corresponds to removal of $5H_2O$ molecules. The last step at two maxima at 256 and 503 °C with weight loss 69.23% (calc.=69.18%) correspond to elimination of $8\,C_2H_2+2CO+2SO_2+5N_2$ giving VSO_4 as a final product. The TG and DTG data of complex (2) proved that the complex completely decomposed in to stages. The first one at 88 °C with weight loss 9.33% (calc.=9.39%) correspond to loss of lattice water molecules. The final step occurs at 176–618 °C with mass loss 62.05% (calc.=62.00%) corresponding to the loss of $5C_2H_2+NH_3+2HCl+2SO_2+0.5H_2+4.5N_2$ and ZrO_2+8C are the final product. The Pd(II) complex decomposed in one step ranged at 25–550 °C with weight loss 84.93% (calc.=85.04%) correspond to loss of $6C_2H_2+2HSCN+4CO+Cl_2+4N_2$ giving Pd as a final product. The TG of Pt(IV) complex proceeds approximately at one step which found with two maxima 295, 527 °C with weight loss 61.67% (calc.=61.31%) corresponding to the loss of $5C_2H_2+2H_2S+4N_2+2NO+2Cl_2$, giving PtO_2+8C as a final residue. The thermal decomposition of complex (5) proceeds via two main degradation steps. The first step occurs at two temperatures maxima 55 and 127 °C, with weight loss 9.10% (calc.=9.16%) attributed to the loss of $5H_2O$. The second step of decomposition occurs at three temperatures maxima 240, 348 and 496 °C with weight loss 63.40% (calc.=63.34%) corresponding to loss $7C_2H_2+4CO+2SO_2+2NO+5N_2$ (*Table 5*).

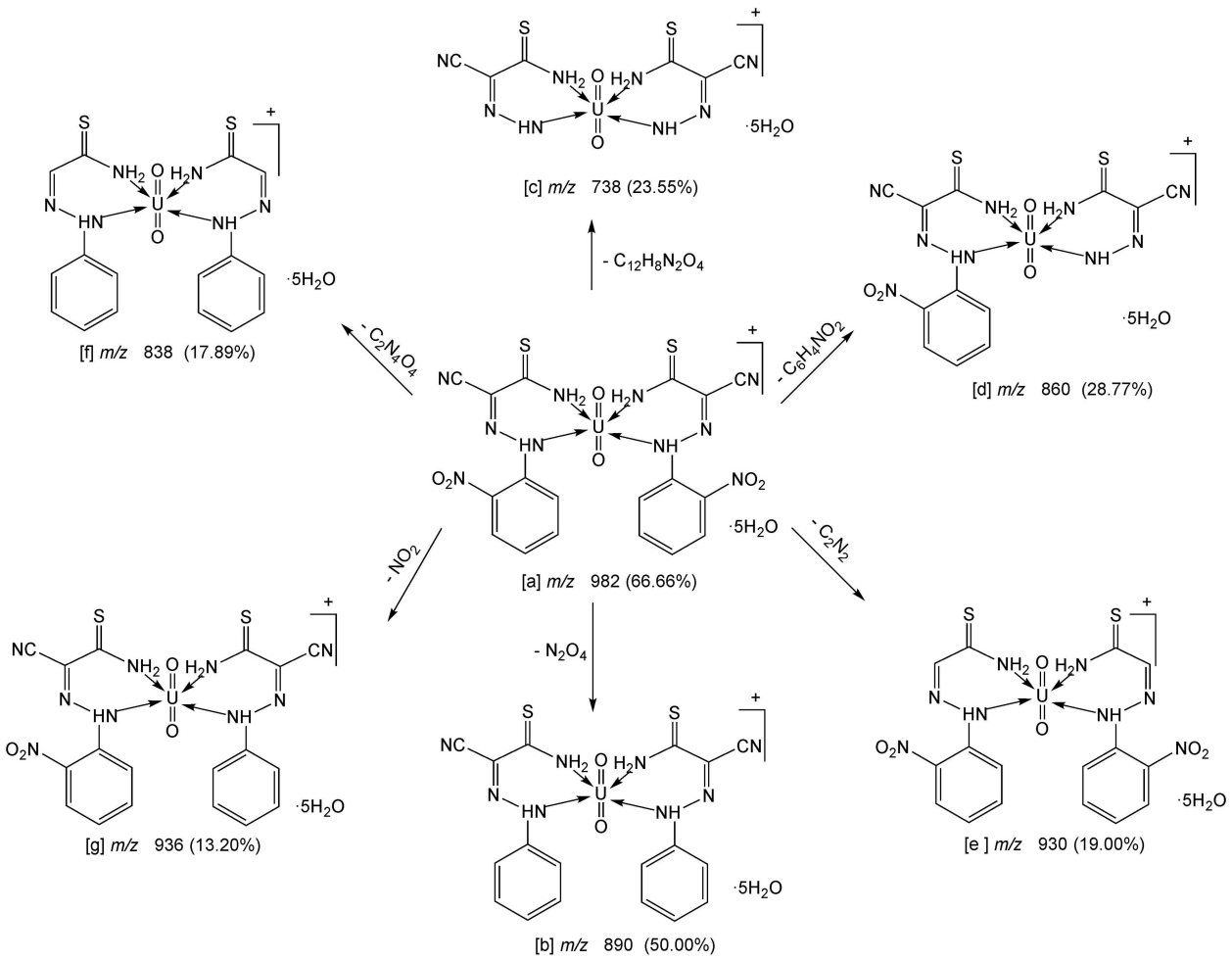

Scheme 2. Fragmentation pattern of complex (**5**).

Table 5. Thermogravimetric data of Cnphta and its metal complexes.

Compounds	TG range (°C)	DTG $_{max}$ (°C)	% Estimated (calculated)		Assignment
			Mass loss	Total mass loss	Lost species
Cnphta	First step	260, 561	99.90 (100.00)	99.90 (100.00)	$HSCN + 3C_2H_2 + 2CO + 2N_2$
1	First step	103	11.67 (11.70)		$5H_2O$
	Second step	256, 503	69.23 (69.18)	81.10 (80.88)	$8C_2H_2 + 2CO + 2SO_2 + 5N_2$
	Residue		19.10 (19.11)		VSO_4
2	First step	88	9.33 (9.39)		$4H_2O$
	Second step	269, 352, 565	62.05 (62.00)	71.38 (71.39)	$5C_2H_2 + NH_3 + 2HCl + 2SO_2 + 0.5H_2 + 4.5N_2$
	Residue		28.62 (28.60)		$ZrO_2 + 8C$
3	First step	383	84.33(84.24)	84.33 (84.24)	$6C_2H_2 + 2HSCN + 4CO + Cl_2 + 4N_2$
	Residue		15.67 (15.75)		Pd
4	First step	295, 527	61.67 (61.31)	61.67 (61.31)	$5C_2H_2 + 2H_2S + 4N_2 + 2NO + 2Cl_2$
	Residue		38.33 (38.68)		$PtO_2 + 8C$
5	First step	55, 127	9.10 (9.16)		$5H_2O$
	Second step	240, 348, 496	63.40 (63.34)	72.50 (72.50)	$7C_2H_2 + 4CO + 2SO_2 + 2NO + 5N_2$
	Residue		27.50 (27.49)		UO_2

Table 6. Thermal behavior and kinetic parameters determined using the Coats–Redfern (CR) and Horowitz–Metzger (HM) operated for Cnphta and its metal complexes.

Compounds	T_s (K)	Method	Parameter					R[a]	SD[b]
			ΔE^* (kJ mol^{-1})	A (s^{-1})	ΔS^* (J mol^{-1} K^{-1})	ΔH^* (kJ mol^{-1})	ΔG^* (kJ mol$^{-1)}$		
Cnphta	533	CR	76.75	3.73×10^{6}	−123.92	72.31	138.35	0.97	0.23
		HM	87.01	6.08×10^{7}	−81.56	82.59	126.06	0.98	0.09
1	776	CR	133.84	2.47×10^{8}	−92.19	127.39	198.93	0.99	0.11
		HM	153.11	3.03×10^{9}	−39.30	146.55	177.05	0.99	0.05
2	837	CR	111.14	6.62×10^{5}	−142.06	104.18	223.08	0.99	0.08
		HM	133.07	2.25×10^{7}	−112.74	126.11	220.00	0.99	0.02
3	656	CR	114.87	1.07×10^{8}	−78.53	109.41	160.92	0.97	0.23
		HM	123.01	1.05×10^{9}	−78.78	96.55	148.22	0.96	0.12
4	568	CR	37.56	1.10×10^{2}	−211.11	32.83	152.74	0.99	0.09
		HM	48.36	2.47×10^{3}	−185.19	43.63	148.81	0.95	0.17
5	769	CR	104.90	8.42×10^{6}	−120.21	98.50	190.94	0.99	0.13
		HM	101.45	7.80×10^{5}	−139.98	95.05	202.69	0.99	0.03

a = correlation coefficients of the Arrhenius plots and b = standard deviation.

Thermodynamic Parameters

The kinetic parameters ΔH*, ΔE*, ΔG* and ΔS* (*Table 6*) were tested using Coats-Redfern and Horowitz-Metzger models equations (Figure S6).[31,32] Decomposition steps of activation energies were found in the range 48.36–153.11 kJ mol^{-1}. The positive sign of ΔG* for complexes demonstrated that the free energy of the final residue's was higher than the initial compounds, implying all decomposition steps non-spontaneous process.[5] For the subsequent decomposition stages of a given complex, the values of the activation, ΔG*, increased significantly. This explained that substantially rising the values of TΔS* from one stage to the next overrides the values of ΔH*. Negative ΔS* values for the degradation process of metal complexes suggested the activated fragments have more ordered structure than reactants or decomposition reactions are slow.[5,33,34]

$$\ln X = \ln\left[\frac{1-(1-\alpha)^{1-n}}{T^2(1-n)}\right] = \ln\left(\frac{AR}{\beta E}\right) - \frac{E_a}{RT} \quad \text{for } n\neq 1 \quad (1)$$

$$\ln X = \ln\left[\frac{-\ln(1-\alpha)}{T^2}\right] = \ln\left(\frac{AR}{\beta E}\right) - \frac{E_a}{RT} \quad \text{for } n = 1 \quad (2)$$

$$\ln[-\ln(1-\alpha)] = \frac{E_a\theta}{RT_s^2} \quad \text{for } n = 1 \quad (3)$$

$$\ln\left[\frac{1-(1-\alpha)^{1-n}}{1-n}\right] = \ln\left(\frac{A}{\beta}\frac{RT_s^2}{E}\right) - \frac{E_a}{RT_s} + \frac{E_a\,\theta}{RT_s^2} \quad \text{for } n\neq 1 \quad (4)$$

$$\Delta H^* = E_a - RT \quad (5)$$

$$\Delta S^* = R\ln\frac{hA}{K_B T} \quad (6)$$

$$\Delta G^* = \Delta H^* - T\Delta S^* \quad (7)$$

Antimicrobial Activity

Cnphta and its complexes were verified for bactericidal effect against two G+ve (*S. aureus* K1 and *B. subtilis* K22) and two G-ve (*E. coli* K32 and *P. aeruginosa* SW1) compared to the positive controls Ampicillin, Amoxycillin and Cefaloxin (Table S1). Whereas the fungicidal activity of the studied compounds were verified against two serious pathogenic fungi (*A. flavus* and *A. fumigatus*) compared to the positive control Ketoconazole (Table S1). The results of antibacterial and antifungal assay were represented in *Figures 3* and *4* where all tested treatments showed remarkable bactericidal and fungicidal activities against all tested pathogens.

The biological activity of the above mentioned complexes can be explained through the Overtone's concept. The antimicrobial activity of the parent ligand can be enhanced by the chelation with the studied

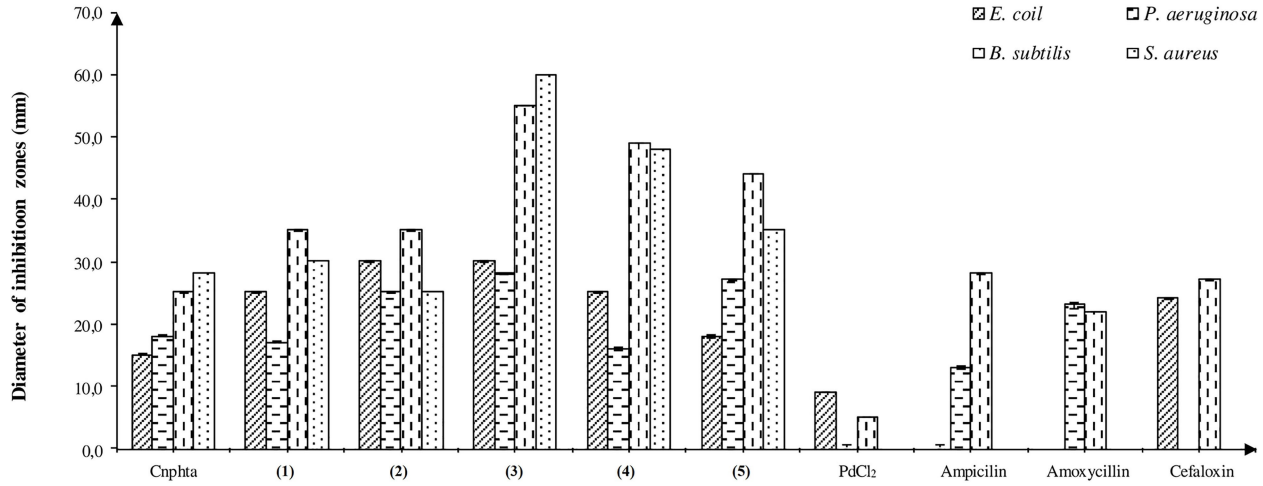

Figure 3. Antibacterial activity of Cnphta and its metal complexes against tested pathogenic bacteria.

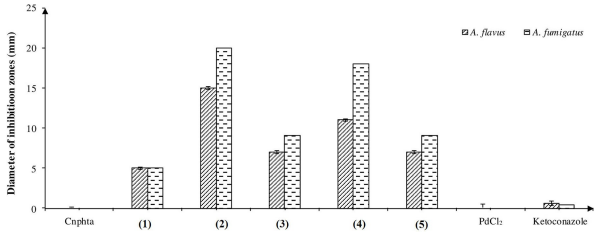

Figure 4. Antifungal activity of Cnphta and its metal complexes against tested phytopathogenic fungi.

metal ions. In particular, the chelation process enhance the delocalization of the electrons increasing the lipophilicity of the central ions and ease the penetration through the microbial cell membrane.[35–37] Furthermore, the increase in lipophilicity aid the tested compounds to penetrate deeper into the microorganisms cells which blocks the metal binding sides of microbial enzymes.[36,38–42] The metal complexes can also disturb the respiration process of the microorganism and block the synthesis of proteins inhibiting the growth of the organism. The antibacterial activity of metal complexes can be ordered as following: (**3**) > (**4**) > (**5**) > (**2**) > (**1**), whereas the antifungal can be ordered as following: (**2**) > (**4**) > (**3**) ≥ (**5**) > (**1**). In all cases the bioactivity of prepared complexes were higher than the parent ligand.

Conclusions

A new hetero organic compound 2-cyano-2-[(2-nitrophenyl)hydrazono]thioacetamide was synthesized and reacted with some metal ions (V(IV), Zr(IV), Pd(II), Pt(IV) and U(VI)) to form the corresponding complexes. The suggested chemical formulae and the probable structures of Cnphta and its metal complexes were supported by elemental analyses, molar conductivity, magnetic, ^{1}H-NMR, MS, IR, UV/VIS and TG measurements. The infrared data indicated that Cnphta chelated with metal ions through two N atoms leading to the formation of octahedral geometries for all complexes except Pd(II) complex which tends to be square planar structure. The data of thermal studies for the compounds supporting the chelation, nature and the number of water in the complexes. Results showed that the tested compounds have noteworthy antimicrobial effect against all tested pathogens especially against *S. aureus*, *B. subtilis* and *A. fumigatus* compared to the positive controls. The chemical structure of the free ligand Cnphta is important factor related to the promising antimicrobial activity of some trace elements. In addition, the metal complexes demonstrated highly significant activities as compared to the single Cnphta ligand. The outcomes of this research indicate the possible use of these new prepared compounds against the new resistant pathogenic strains to the commonly used antibiotics or fungicides.

Experimental Section

Chemicals

All chemicals used were of the analytical reagent grade (AR) and of highest purity and are commercially from different sources. $VOSO_4 \cdot H_2O$ (99.9%), $ZrOCl_2 \cdot 8H_2O$ (99.9%), $PdCl_2$ (99.9%), $PtCl_4$ (99.9%) and

$UO_2(NO_3)_2 \cdot 6H_2O$ (99.9%) (Aldrich Chemical Co.). Yeast extract and agar (Sigma) were also used and all solvents were purchased from Fluka Chemical Co.

Synthesis of Cnphta

Cnphta was prepared by dissolving 5 mmol (0.5 g) of 2-cyanoethanethioamide (**A**) in 20 mL ethanol and 5 mmol (0.9275 g) of 2-nitrobenzene diazonium chloride (**B**) in 30 mL ethanol in presence of CH_3COONa in 1:1 molar ratio and cooled to 0 °C on ice bath (*Scheme 3*). The resulting solid was filtered, dried and purified by recrystallization from ethanol to afford compound.

Synthesis of Metal Complexes

The dark-brown solid complex $[VO(Cnphta)_2(H_2O)]SO_4 \cdot 5H_2O$ (**1**) was prepared by addition of $VOSO_4 \cdot H_2O$ (0.5 mmol, 0.091 g) in 20 mL acetone to Cnphta (1 mmol, 0.25 g) in 20 mL acetone. The reaction mixture was stirred at room temperature for 24 h. The mixture was left for slow evaporation, then the formed precipitate as filtered off, washed several times using bidistilled water and dried over $CaCl_2$ in a desiccator. Whereas, yellowish-white $[ZrO(C_9H_7N_5O_2S)_2(H_2O)]Cl_2 \cdot 4H_2O$ (**2**), black $[Pd(C_9H_7N_5O_2S)_2]Cl_2$ (**3**), orange-brown $[Pt(C_9H_7N_5O_2S)_2Cl_2]Cl_2$ (**4**) and yellowish-green $[UO_2(C_9H_7N_5O_2S)_2](NO_3)_2 \cdot 5H_2O$ (**5**) solid complexes were synthesized as mentioned previously, utilizing acetone as a solvent and corresponding metal salts, respectively, in 1:2 molar ratios (M:Cnphta).

Instruments

C, H and N were done elemental experiments via a Perkin Elmer 2400 CHN elemental analyzer. The proportion of metal ions was gravimetrically measured by transforming solid compounds into metal, metal salt or metal oxide and using the atomic absorption technique (Spectrometer-PYE-UNICAM SP 1900).[5,6] FT-IR spectra in KBr discs were enrolled from 4000–400 cm^{-1} with FT-IR 460 PLUS Spectrophotometer. ^{1}H-NMR spectra have been registered on Varian Mercury VX-300 NMR Spectrometer utilizing (D_6)DMSO as solvent. TG-DTG processes were conducted out under nitrogen atmospheric conditions within range from room temperature to 800 or 1000 °C using TGA-50H Shimadzu and the sample weight was precisely weighted in an aluminum crucible. Electronic spectra were obtained using UV-3101PC Shimadzu. The solid reflection spectra were done as potassium bromide pellets. The mass spectra were run at GCMS-QP-1000EX Shimadzu (ESI-70ev) in the range from 0–1090. Magnetic Susceptibilities were determined on a Sherwood Scientific Magnetic Susceptibility Balance (Model MKI) at room temperature using $Hg[Co(SCN)_4]$ as a calibrant; diamagnetic corrections were calculated from Pascal's constant. Melting points have been transcribed on the Buchi apparatus. The molar conductivity of Cnphta and its metal complexes in dimethyl formamide (1×10^{-3} M) was evaluated using CONSORT K410.

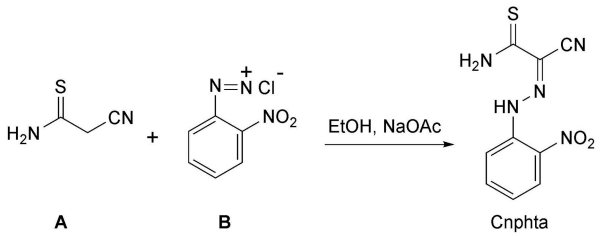

Scheme 3. Synthesis of Cnphta.

Antimicrobial Investigation

Tested Bacterial Strains

The tested bacterial strains, *S. aureus* K1, *B. subtilis* K22 (G+ve) and *E. coli* K32 and *P. aeruginosa* (G-ve) have been conserved as pure cultures in the collection of the School of Agricultural, Forestry, Food and Environmental Sciences (SAFE), University of Basilicata, Potenza, Italy.

Tested Fungal Strains

The tested phytopathogenic fungi, *A. flavus* and *A. fumigatus*, were stored as pure cultures at 4 °C on potato dextrose agar (PDA) in the mycotheca of SAFE, University of Basilicata, Potenza, Italy. Both tested fungi were previously identified using morphological and molecular methods. The genomic DNA (gDNA) of each tested fungi was extracted using a Qiagen Genomic DNA Kit (Qiagen, Heidelberg, Germany). The extracted gDNA was amplified using TS4 and TS5 primers[43,44] and the obtained amplicons were sequenced and matched to those present in GenBank using Simple Local Alignment Search Tool program from 1990 (BLAST, USA).[45]

Microbicidal Assay

The antibacterial and antifungal activity of all tested compounds (**1**), (**2**), (**3**), (**4**) and (**5**) were examined following the method of Beecher and Wong process[46] with minor modifications. Briefly, the Mueller-Hinton culture media was prepared and was inoculated with each tested pathogen. Five mm diameter holes were drilled with a sterile cork-borer on surface media. One hundred μL of each tested compounds, after completely dissolved in DMSO at 10^{-3} M, were injected into holes and then all plates were incubated at 37 °C for 20 h for bacteria and 7 days at 30 °C for fungi. The antimicrobial activity was estimated by measuring the diameter of inhibition zone (mm ± SDs) compared to Ampicilin, Amoxycillin and Cefaloxin as positive controls for bactericidal assay and Ketoconazole for fungi.

Acknowledgements

The authors gratefully acknowledge Zagazig University, Egypt for the support of this research work. Open Access Funding provided by Universita degli Studi della Basilicata within the CRUI-CARE Agreement.

Author Contribution Statement

M.S. El-Attar: Formal analysis, Data curation, Investigation. Writing - review & editing. H.S. Elshafie: Investigation, Data curation, Writing - review & editing, Supervision. S.A. Sadeek: Data curation, Writing – review& editing, Supervision. A.F. El-Farargy: Data curation, Writing - review & editing, Supervision. S.I. El-Desoky: Methodology, Formal analysis, Data curation, Investigation. W.H. El-Shwiniy: Methodology, Formal analysis, Data curation, Investigation. I. Camele: Data curation, Writing - review & editing, Supervision.

References

[1] F. M. Abdelrazek, N. H. Metwally, 'Novel Synthesis of N-Arylpyrrole, Pyrrolo[1,2-a]quinazoline and Pyrrolo[3,4-d] pyridazine Derivatives', *Synth. Commun.* **2009**, *39*(22), 4088–4099.

[2] F. M. Abdelrazek, P. Metz, O. Kataeva, A. Jäger, S. F. El-Mahrouky, 'Synthesis and Molluscicidal Activity of New Chromene and Pyrano[2,3-c]pyrazole Derivatives', *Arch. Pharm. Chemi* **2007**, *340*(10), 543–548.

[3] F. M. Abdelrazek, A. A. Fadda, A. N. Elsayed, 'Novel Synthesis of Some New Pyridazine and Pyridazino[4,5-d] pyridazine Derivatives', *Synth. Commun.* **2011**, *41*(8), 1119–1126.

[4] F. M. Abdelrazek, P. Metz, N. H. Metwally, S. F. El-Mahrouky, 'Synthesis and Molluscicidal Activity of New Cinnoline and Pyrano[2,3-c] pyrazole Derivatives', *Arch. Pharm. Chemi* **2006**, *339*(8), 456–460.

[5] W. H. El-Shwiniy, A. G. Ibrahim, S. A. Sadeek, W. A. Zordok, 'Synthesis, structural elucidation, molecular modeling and antimicrobial studies of 6-(2-hydroxyphenylimine)-2-thioxotetrahydropyrimidin-4(1H)-one (L) Schiff base metal complexes', *Appl. Organomet. Chem.* **2021**, *35*, e6174.

[6] S. A. Sadeek, S. M. Abd El-Hamid, A. A. Mohamed, W. A. Zordok, H. A. El-Sayed, 'Spectroscopic characterization, thermogravimetry, density functional theory and biological studies of some mixed- ligand complexes of meloxicam and 2,2′-bipyridine with some transition metals', *Appl. Organomet. Chem.* **2019**, *33*, e4889.

[7] A. A. Fadda, F. M. Abdelrazek, K. S. Mohamed, H. M. M. Ghieth, H. A. Etman, 'Synthetic Applications of Benzothiazole Containing Cyanoacetyl Group', *Eur. J. Chem.* **2010**, *1*(2), 90–95.

[8] L. Chrzastek, B. Mianowsk, W. Sliwa, 'Synthesis and Properties of Methyl-, Formyl- and Amino-Diazaphenanthrene', *Aust. J. Chem.* **1994**, *47*, 2129–2133.

[9] E. Tfouni, M. Krieger, B. R. McGarvey, D. W. Franco, 'Structure, chemical and photochemical reactivity and biological activity of some ruthenium amine nitrosyl complexes', *Coord. Chem. Rev.* **2003**, *236*(1-2), 57–69.

[10] C. P. Montgomery, B. S. Murray, E. J. New, R. Pal, D. Parker, 'Cell-Penetrating Metal Complex Optical Probes: Targeted and Responsive Systems Based on Lanthanide Luminescence', *Acc. Chem. Res.* **2009**, *42*(7), 925–937.

[11] M. Tsaramyrsi, M. Kaliva, A. Salifoglou, C. P. Raptopoulou, A. Terzis, V. Tangoulis, J. Giapintzakis, 'Vanadium(IV)-Citrate Complex Interconversions in Aqueous Solutions. A pH-Dependent Synthetic, Structural, Spectroscopic, and Magnetic Study', *Inorg. Chem.* **2001**, *40*(23), 5772–5779.

[12] I. Muhammad, I. Javed, I. Shahid, I. Nazia, 'In Vitro Antibacterial Studies of Ciprofloxacin-imines and Their Complexes with Cu(II), Ni(II), Co(II), and Zn(II)', *Turk. J. Biol.* **2007**, *31*, 67–72.

[13] A. J. Florence, A. R. Kennedy, N. Shankland, E. Wright, A. Al-Rubayi, 'Norfloxacin dehydrate', *Acta Crystallogr. Sect. C* **2000**, *56*, 1372–1373.

[14] I. Turel, P. Bukovec, M. Quirós, 'Crystal structure of ciprofloxacin hexahydrate and its characterization', *Int. J. Pharm.* **1997**, *152*(1), 59–65.

[15] A. S. shmidevi, K. Vyas, G. Om Reddy, 'Sparfloxacin, an antibacterial drug', *Acta Crystallogr. Sect. C* **2000**, *56*, e115-e116.

[16] W. J. Geary, 'The use of conductivity measurements in organic solvents for the characterisation of coordination compounds', *Coord. Chem. Rev.* **1971**, *7*(1), 81–122.

[17] S. S. Qian, X. S. Cheng, Z. L. You, H. L. Zhu, 'Synthesis and Crystal Structures of Ethanol-Coordinated Molybdenum (VI) Oxo Complexes with Tridentate Hydrazone Ligands', *Acta Chim. Slov.* **2013**, *60*(4), 870–874.

[18] S. A. Sadeek, W. H. EL-Shwiniy, 'Preparation, structure and microbial evaluation of metal complexes of the second generation quinolone antibacterial drug lomefloxacin', *J. Mol. Struct.* **2010**, *981*(1-3), 130–138.

[19] R. P. Feazell, N. N. Ratchford, H. Dai, S. J. Lippard, 'Soluble single-walled carbon nanotubes as longboat delivery systems for platinum (IV) anticancer drug design', *J. Am. Chem. Soc.* **2007**, *129*(27), 8438–8439.
[20] S. A. Al-Shihri, 'Synthesis, characterization and thermal analysis of some new transition metal complexes of a polydentate Schiff base', *Spectrochim. Acta Part A* **2004**, *60*(5), 1189–1192.
[21] E. M. Nour, I. S. Alnami, N. A. Alem, 'Spectroscopic studies on the uranyl-schiff base solid complex (N, N′-p-phenyl-enebis (salicylideneiminato) UO2)', *J. Phys. Chem. Solids* **1992**, *53*(1), 197–201.
[22] W. H. El-Shwiniy, W. S. Shehab, W. A. Zordok, 'Spectral, thermal, DFT calculations, anticancer and antimicrobial studies for bivalent manganese complexes of pyrano [2, 3-d] pyrimidine derivatives', *J. Mol. Struct.* **2020**, *1199*, 126993.
[23] W. H. El-Shwiniy, W. A. Zordok, 'Synthesis, spectral, DFT modeling, cytotoxicity and microbial studies of novel Zr(IV), Ce(IV) and U(VI) piroxicam complexes', *Spectrochim. Acta Part A* **2018**, *199*, 290–300.
[24] S. P. McGlynn, J. K. Smith, W. C. Neely, 'Electronic structure, spectra, and magnetic properties of oxycations. III. Ligation effects on the infrared spectrum of the uranyl ion', *J. Chem. Phys.* **1961**, *35*(1), 105–116.
[25] L. H. Jones, 'Determination of UO bond distance in uranyl complexes from their infrared spectra', *Spectrochim. Acta.* **1959**, *15*, 409–411.
[26] W. H. EL-Shwiniy, S. A. Sadeek, 'Synthesis and characterization of new 2-cyano-2-(p-tolylhydrazono)thioacetamide metal complexes and a study on their antimicrobial activities', *Spectrochim. Acta Part A* **2015**, *137*, 535–546.
[27] K. Nakamoto, P. J. McCarthy, S. Fujiwara, Y. Shimura, J. Fujita, C. R. Hare, Y. Saito, ' *Spectroscopy and structure of metal chelate compounds*, Ch. 2, John Wiley & Sons, New York, London, Sydney, **1968**.
[28] M. Saif, M. M. Mashaly, M. F. Eid, R. Fouad, 'Synthesis, characterization and thermal studies of binary and/or mixed ligand complexes of Cd(II), Cu(II), Ni(II) and Co(III) based on 2-(Hydroxybenzylidene) thiosemicarbazone: DNA binding affinity of binary Cu(II) complex', *Spectrochim. Acta Part A* **2012**, *92*, 347–356.
[29] W. H. El-Shwiniy, W. S. Shehab, S. F. Mohamed, H. G. Ibrahium, 'Synthesis and cytotoxic evaluation of some substituted pyrazole zirconium (IV) complexes and their biological assay', *Appl. Organomet. Chem.* **2018**, *32*(10), e4503.
[30] T. Skauge, I. Turel, E. Sletten, 'Interaction between Ciprofloxacin and DNA Mediated by Mg2+-ions', *Inorg. Chem.* **2002**, *339*, 239–247.
[31] A. W. Coats, J. P. Redfern, 'inetic parameters from thermogravimetric data', *Nature* **1964**, *201*, 68–69.
[32] H. H. Horowitz, G. Metzger, 'A new analysis of thermogravimetric traces', *Anal. Chem.* **1963**, *35*, 1464–1468.
[33] M. Dolaz, V. McKee, A. Golcu, M. Tumer, 'Synthesis, Structural Characterization, Spectroscopic and Electrochemical Studies of N,N′-bis[(2,4-dimethoxyphenyl) methylidene]butane-1,4-diamine', *Curr. Org. Chem.* **2010**, *14*(3), 281–288(8).
[34] A. Gölcü, M. Dolaz, H. Demirelli, M. Diðrak, S. Serin, 'Spectroscopic and Analytic Properties of New Copper(II) Complex of Antiviral Drug Valacyclovir', *Transition Met. Chem.* **2006**, *31*(5), 658–665.
[35] S. H. Sakr, H. S. Elshafie, I. Camele, S. A. Sadeek, 'Synthesis, spectroscopic, and biological studies of mixed ligand complexes of gemifloxacin and glycine with Zn(II), Sn(II), and Ce(III)' *Molecules* **2018**, *23*(1182), 1–17.
[36] Z. H. Chohan, K. M. Khan, C. T. Supuran, 'Synthesis of antibacterial and antifungal cobalt(II), copper(II), nickel(II) and zinc(II) complexes with bis-(1,1′-disubstituted ferrocenyl)thiocarbohydrazone and bis-(1,1′-disubstituted ferrocenyl)carbohydrazone', *Appl. Organomet. Chem.* **2004**, *18*(7), 305–310.
[37] R. Maruvada, S. C. Pal, N. G. Balakrish, 'Effects of polymyxin B on the outer membranes of Aeromonas species', *J. Microbiol. Methods* **1994**, *20*(2), 115–124.
[38] H. S. Elshafie, S. A. Sadeek, W. A. Zordok, A. A. Mohamed, 'Meloxicam and Study of Their Antimicrobial Effects against Phyto and Human Pathogens', *Molecules* **2021**, *26*(5), 1480.
[39] A. A. Mohamed, H. S. Elshafie, S. A. Sadeek, I. Camele, 'Biochemical Characterization, Phytotoxic Effect and Antimicrobial Activity against Some Phytopathogens of New Gemifloxacin Schiff Base Metal Complexes', *Chem. Biodiversity* **2021**, *18*(9), e2100365.
[40] A. M. Beltagi, 'Determination of the antibiotic drug pefloxacin in bulk form, tablets and human serum using square wave cathodic adsorptive stripping voltammetry', *J. Pharm. Biom. Anal.* **2003**, *31*(6), 1079–1088.
[41] S. M. Abd El-Hamid, S. A. Sadeek, W. A. Zordok, W. H. El-Shwiniy, 'Synthesis, spectroscopic studies, DFT calculations, cytotoxicity and antimicrobial activity of some metal complexes with ofloxacin and 2,2′-bipyridine', *J. Mol. Struct.* **2019**, *1176*, 422–433.
[42] B. G. Tweedy, 'Plant extracts with metal ions as potential antimicrobial agents', *Phytopathology* **1964**, *55*, 910–918.
[43] T. J. White, T. Bruns, S. Lee, J. Taylor, 'Amplification and Direct Sequencing of Fungal Ribosomal RNA Genes for Phylogenetics. In: M. A. Innis, D. H. Gelfand, J. J. Sninsky, T. J. White, Eds., PCR protocols. A Guide to Methods and Applications', *Academic Press*, San Diego, CA, USA, **1990**, 315–322.
[44] I. Camele, C. Marcone, G. Cristinzio, 'Detection and identification of Phytophthora species in southern Italy by RFLP and sequence analysis of PCR-amplified nuclear ribosomal DNA', *Eur. J. Plant Pathol.* **2005**, *113*, 1–14.
[45] S. F. Altschul, T. L. Madden, A. A. Schaffer, J. Zhang, Z. Zhang, W. Miller, D. J. Lipman, 'Gapped BLAST and PSIBLAST: a new generation of protein database search programs', *Nucleic Acids Res.* **1997**, *25*, 3389–3402.
[46] D. J. Beecher, A. C. Wong, 'Identification of hemolysin BL-producing *Bacillus cereus* isolates by a discontinuous hemolytic pattern in blood agar', *Appl. Environ. Microbiol.* **1994**, *60*(5), 1646–1651.

Received September 28, 2021
Accepted December 6, 2021